Hindawi Publishing Corporation
Advances in Condensed Matter Physics
Volume 2015, Article ID 297363, 6 pages
http://dx.doi.org/10.1155/2015/297363

Research Article

Core Microstructure and Strain State Analysis in MgB_2 Wires with Different Metal Sheaths

C. E. Sobrero,[1] M. T. Malachevsky,[1,2] and A. Serquis[1,2]

[1]*Centro Atómico Bariloche, CNEA, Avenida Bustillo 9500, 8400 San Carlos de Bariloche, Argentina*
[2]*CONICET, 8400 San Carlos de Bariloche, Argentina*

Correspondence should be addressed to C. E. Sobrero; cesarsobrero@hotmail.com

Received 11 December 2014; Revised 18 February 2015; Accepted 25 February 2015

Academic Editor: Veer P. S. Awana

We present a detailed analysis of the effect of the sheath materials on the microstructure and superconducting properties of MgB_2 wires produced by the powder-in-tube method (PIT). We reduced commercial MgB_2 powder by attrition milling in nitrogen atmosphere using tungsten carbide balls and obtained powders with grain sizes lower than 150 nm and different strain states through this process. Several Ti, stainless steel, and copper monofilamentary wires were prepared using these powders by the PIT method. We investigated different thermal treatments and mechanical paths during the processing of the wires for the enhancement of the critical currents. The superconducting properties were determined by magnetization measurements in a SQUID magnetometer. The correlation between the thermal treatments, structure, and superconducting properties is discussed.

1. Introduction

The superconducting critical temperature (T_c) of this binary compound makes MgB_2 [1] attractive for cryogenic liquid-free technological applications. Some of the advantages of MgB_2 are its low cost and low weight and the absence of weak links at the grain boundaries. Since its discovery, a remarkable progress has been done in increasing the critical current densities (J_c) by optimizing processing parameters. The powder-in-tube (PIT) method has been preferred early on by several groups to prepare MgB_2 wires or tapes. The best results for increasing J_c and irreversibility field (H_{irr}) in bulk samples are related to an improvement in grain connectivity [2] but also to the addition of suitable defect nanoparticles or doping, for example, $Mg(B_{1-x}O_x)_2$ [3], SiC [4, 5].

Grain connectivity is more relevant for MgB_2 wires and tapes required for applications, in which fabrication and processing conditions strongly affect microstructures and current carrying capability. The standard and low-cost fabrication PIT method involves filling a metallic tube with superconducting powder (ex situ) or precursors (in situ) and drawing it into a wire and/or rolling into a tape [6]. MgB_2 crystallizes in the hexagonal AlB_2 type structure (space group P6/mmm), and the anisotropic structure has given the motivation to investigate the presence of texture induced by different deformation processes. A key issue on which there is no agreement in the literature is the optimization of the heat treatment parameters. Although some postannealing appears to be necessary to achieve higher J_c, some authors reported detrimental effects of heat treatments on the performance of MgB_2 wires or tapes [2, 6]. In the present work we review the results obtained in MgB_2 wires prepared by PIT using metal sheaths of different hardness: stainless steel, copper, or titanium, to establish a relationship among annealing conditions, modifications in the microstructure, and changes in J_c.

2. Experimental

Starting from commercial MgB_2 powder (−325 mesh, 98% Alfa Æsar), we further reduced the agglomerates by attrition milling in nitrogen atmosphere to minimize oxidation, using tungsten carbide as milling media as detailed in earlier works [6, 7], named as-prepared condition from here on. Crystallite size and microstrain within the grains were estimated by powder X-ray diffraction (XRD) and transmission electron microscopy (TEM) measurements. To prepare the wires we

used the ex situ variant of the PIT method. The powder was packed into copper (Cu), stainless steel 316 (SS), and titanium grade 2 (Ti) tubes (inner and outer diameters ~ 4.5 and 6.4 mm and 10 cm long for all sheaths) and cold-drawn into round wires with external diameters in the range of 1.3–1.5 mm, with different intermediate treatments (IT) according to the sheath material. Copper wires were cold-drawn to final shape with a 5 min IT at 500°C, Ti wires needed a 15 min IT at 500°C every 20% cold-drawn reduction step, and SS needed a 40 min IT at 550°C every 15% cold drawn reduction step.

For the samples SS-SiC, 5 at.% SiC nanopowder (20–30 nm grain size) was added to the milled MgB_2 and the mixture was ball-milled for one hour inside a glove-box before filling the SS tube. All samples, except the titanium one, had a final heat treatment at 800°C during one hour under Ar + 5% H atmosphere (HT). For the Ti wires the chosen atmosphere for the HT was pure Ar in order to avoid the hydrogen embrittlement of the sheath.

After the mechanical processing of the different wires, the final lengths vary between 2 and 2.5 m (the longest corresponding to the Cu sheath). In order to avoid some edge effect the final heat treatment was performed on 5 to 10 cm long samples obtained from the center of the wires.

XRD data were collected using a Panalytical Empyrean powder diffractometer using CuKα radiation. Sample surface morphology and microstructures were investigated using a SEM Phillips 515 equipped with an X-ray energy dispersive spectrometer (EDS) and a Phillips CM200UT TEM operating at 200 kV, using a double tilt specimen holder.

A quantum design SQUID magnetometer was used to investigate the dc magnetization, M, of bulk, powder, and wire samples. M versus temperature (T) was measured at magnetic field $H = 30$ Oe after zero field cooling (ZFC) and field cooling (FC). Magnetization loops $M(H)$ were measured between 5 K and 42 K (i.e., slightly above the T_c of MgB_2). When measuring PIT wires the 40 K loops were used to subtract the stainless steel contribution. From the superconducting contribution of the 5 and 20 K loops the magnetic J_c was calculated using the Bean critical state model.

3. Results and Discussion

Figure 1 shows the XRD pattern of the MgB_2 powders in as-prepared condition and extracted from SS wires before and after the final HT. In all the powders the MgB_2 is the major phase, and there also is a small amount of MgO. Some extra peaks were detected on the XRD pattern, related to a small amount of WC contamination from the milling media. The XRD patterns of the powders extracted from Ti and Cu wires presented a similar behavior and are not shown.

The structural parameters as grain size, lattice parameter, and powder strain were obtained from the XRD data using Fullprof, a program based on Rietveld refinement. With this program, the upper limit of the lattice strain within the grains (ε) is obtained using the integral breadths method:

$$\varepsilon = \frac{\beta\lambda}{4\sin\theta} \quad (1)$$

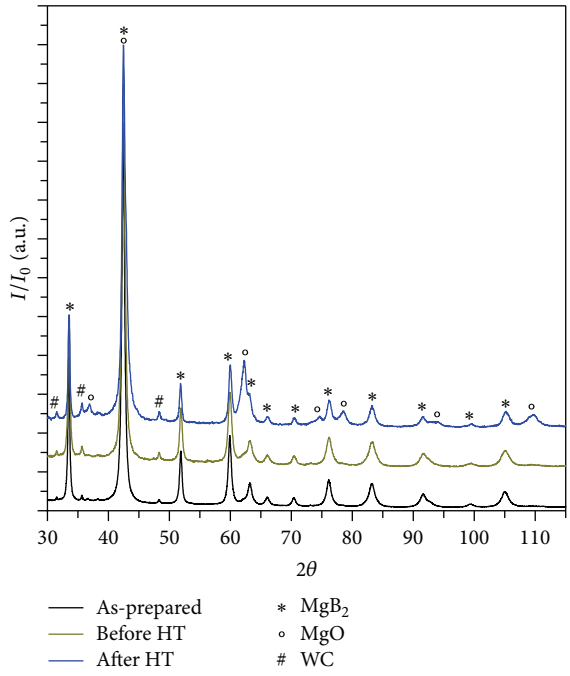

Figure 1: XRD patterns of the MgB_2 powders.

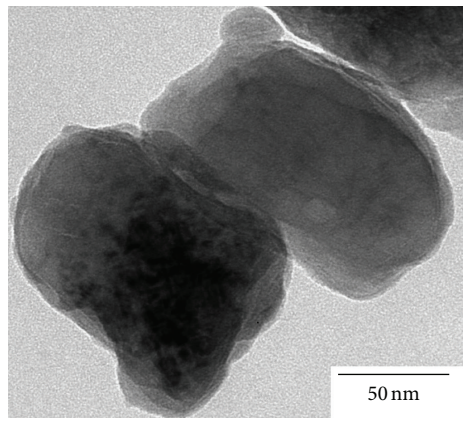

Figure 2: TEM micrograph of the MgB_2 powder in as-prepared condition.

with β being the distortion integral breadth, θ the position of the peak maximum, and λ the wave length. The crystallite size is obtained from the inverse of the pure integral breadth.

The grain size obtained for the as-prepared MgB_2 in as-prepared condition was of 115 nm with a strain of 6.1×10^{-3}. Figure 2 shows a TEM micrograph of the same powder, with some particles of different sizes and noticeably dislocated. The measured grain sizes showed an average grain size of 150 nm with a dispersion around 40 nm taking into account that particles are elongated (not spherical shape), in a good agreement with the value obtained from XRD.

It is known that good superconducting properties on PIT ex situ wires need a high packing density [4]. During the filling of the tube the small particle size allowed us to obtain

a relative density of around 55% of MgB_2 density improving the grain connectivity before cold drawing.

Figure 3 shows the cross-sections of the 4 monofilamentary wires after the final thermal treatment. Figures 3(a) to 3(d) show four low magnification micrographs of the wires, while the second one presents a detail of each superconducting core. Figures 3(a) to 3(d) show no evidence of reaction layer between the superconducting core and any of the sheaths. The hardness of the sheath has a strong influence on the compaction of the superconducting core. For the present sheaths it varies from 50 Vickers for Cu, 150 for Ti, and 175 for SS. The area ratio of the superconducting core varies from 53% for Cu, 48% for Ti, and 46% for SS wires. Figures 3(g) and 3(h) illustrate details of the superconducting cores of SS wires, presenting better connectivity between grains and less pores. Figures 3(e) and 3(f) exhibit the morphology of agglomerated particles with a higher density of pores.

Figure 4 shows the dependence of the J_c of the MgB_2 wires with magnetic field, at different temperatures. The J_c values were determined applying the Bean critical state model [8] to the magnetization loops $M(H)$. The J_c's obtained from SQUID measurements mainly depend on the MgB_2 microstructure and purity and the effect of the different sheaths is not so clear as it should be in a transport J_c measurement, where grain connectivity and core density are involved. Figure 4(a) shows and displays the J_c values of the wires before HT at 5 and 20 K. The J_c behavior is quite similar for all the wires in almost the entire H range; even at 0T self-field the values of 5 and 20 K are nearly almost the same. While there are some compaction differences on the less porous wires among the SS samples, the J_c response of the pretreated samples does not show a variation that can be attributed to this improvement. However, after the final thermal treatment (HT) the J_c response (Figure 4(b)) presents a major difference between the SS samples and the other wires.

The J_c of Cu sheathed wires has lower response values in the whole range compared to the other sheaths. For the Cu samples the SEM-EDS and XRD analyses show no presence of reaction interface after the HT so the lower response can be attributed to the lower compaction observed in Figures 3(a) and 3(e).

J_c values of SS and SS-SiC wires at 5 and 20 K at lower field ($H < 1T$) remain similar to the values for the Ti and Cu wires. However for higher fields the J_c's of SS and SS-SiC show a plateau with values around 10^4 A/cm^2 and 10^3 A/cm^2 for 5 and 20 K. These improvements could be related to flux pinning due to the presence of some defects dispersed on the superconducting core [9]. However, the influence of SiC on the J_c response is not observed. In the ex situ process it is necessary for higher HT temperatures (900 or above) to promote the possible reaction between some C-additives and MgB_2 to create effective pinning centers [10, 11]. In particular, it was reported that flux pinning was enhanced by the carbon substitution for B with increasing sintering temperature [12] which justify that we could not see any effect of SiC addition at the chosen HT low temperatures.

Table 1: Oxygen occupancy on HT powder.

Element	Occ-SS	Occ-Ti
B	1.75	1.74
O	0.25	0.26

In order to evaluate the presence of defects, powders from the different superconducting cores were extracted and observed with a TEM. Figure 5 shows TEM micrographs of the Cu, Ti, SS, and SS-SiC powders. In all the samples, the dislocation density has diminished in comparison to the as-prepared condition powders. The lattice strain of the powders after the HT obtained from XRD has fallen from 6.1×10^{-3} for the as-prepared powder to 4.5×10^{-3} and 5.0×10^{-3} for the Ti and SS wires, respectively. The HT temperature was intentionally kept at lower values, when it is compared with other works to avoid the formation of a reaction layer with the Cu sheath or even with the SS [13]. However as is reported in this work the used heat treatment was successful in reducing the powder's strain state.

A large number of precipitates with diameters between 4 and 15 nm are observed within the MgB_2 crystallite in all TEM images, except for Figure 5(a). The presence of precipitates in a superconducting material can help the vortex pinning [14] by reduction or suppression of the condensation energy within their volume. EDX measurements on TEM were made in order to analyze the precipitates composition. However, due to the small precipitate size, the influence of the matrix is always present on the analysis. The precipitate shows O, Mg, and B for the SS, Ti, and SS-SiC samples. According to a previous work by Liao et al. [3] the composition of the precipitates could be of the $Mg(B,O)_2$ type. The oxygen in these samples may originate from the gases used for the final heat treatment or some MgO in the initial powder. Oxygen solubility in MgB_2 varies with temperature and is higher at 800°C than at room temperature. When the samples are cooled down the extra oxygen is being forced into the MgB_2 matrix and could form the $Mg(B,O)_2$ in the more compact samples [15].

In order to evaluate this possibility, Rietveld analyses were made on the heat treated samples of SS, SS-Sic, and Ti allowing for the variation of oxygen content on the boron site. Table 1 shows the oxygen occupancy on the MgB_2 site from the SS and Ti wires, and the R-factors of the analyzed diffractograms are 2.34 and 2.62. The values for the other SS sample (SS-SiC) show a similar value for the boron occupancy. The calculated values shown on Table 1 allow assuming that the precipitates can be of the $Mg(B,O)_2$ type.

In order to evaluate the influence of these defects on the J_c response of the SS, SS-SiC, and Ti powders we determine their density on the powders. For precipitates with the previous mentioned size range and assuming a spherical shape, the density is around 6×10^{17} precipitates/cm^3 for SS and SS-SiC powder and 5×10^{16} precipitates/cm^3 for the Ti ones. The difference in the precipitate density values is related to the number of IT performed on each wire (almost a 30% more of treatments for SS wires). Also the SS wires needed higher temperatures and longer times for the IT treatments.

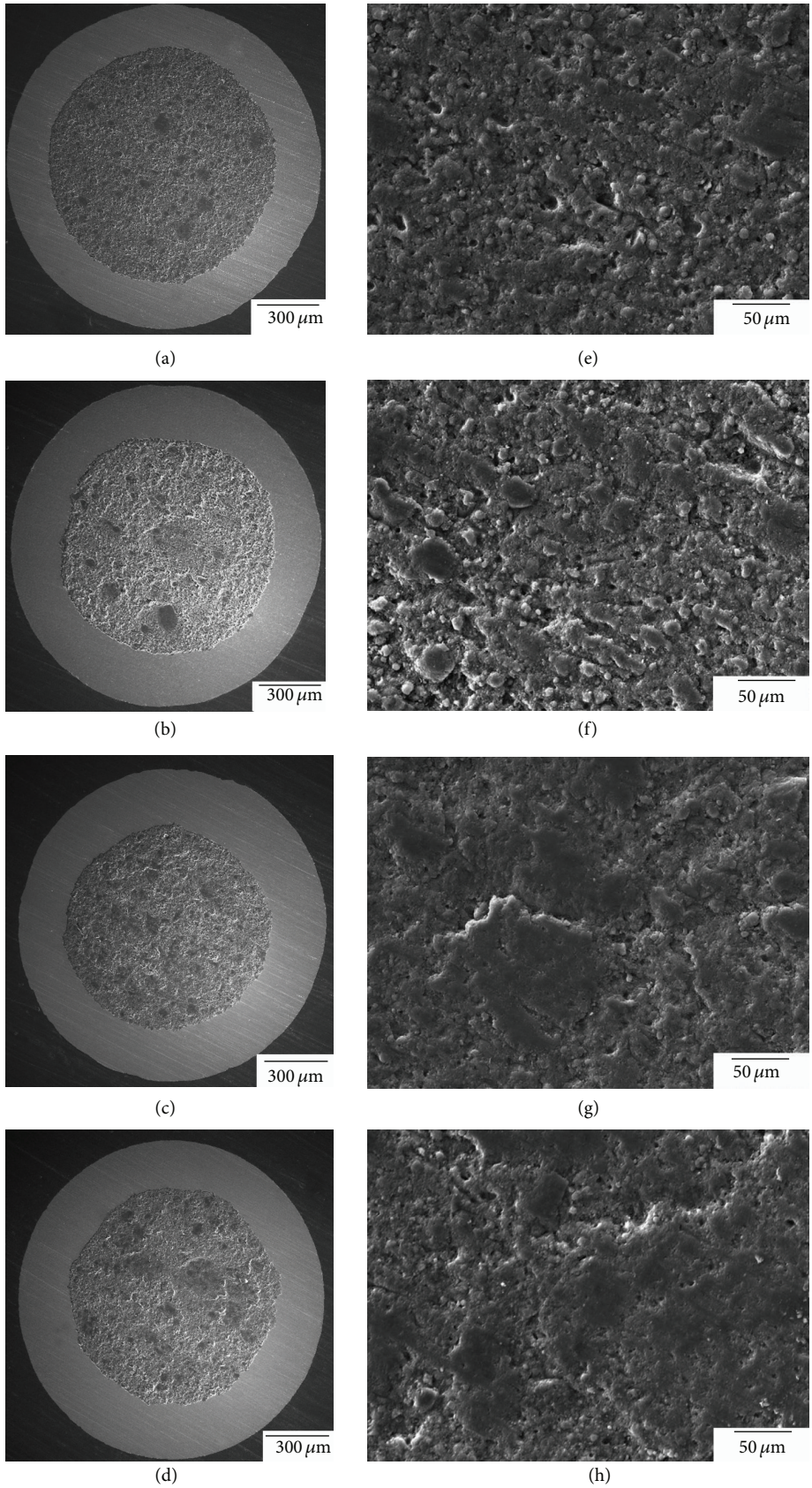

Figure 3: SEM micrographs of the HT wires: (a) and (e) copper, (b) and (f) titanium, (c) and (g) SS, and (d) and (h) SS-SiC.

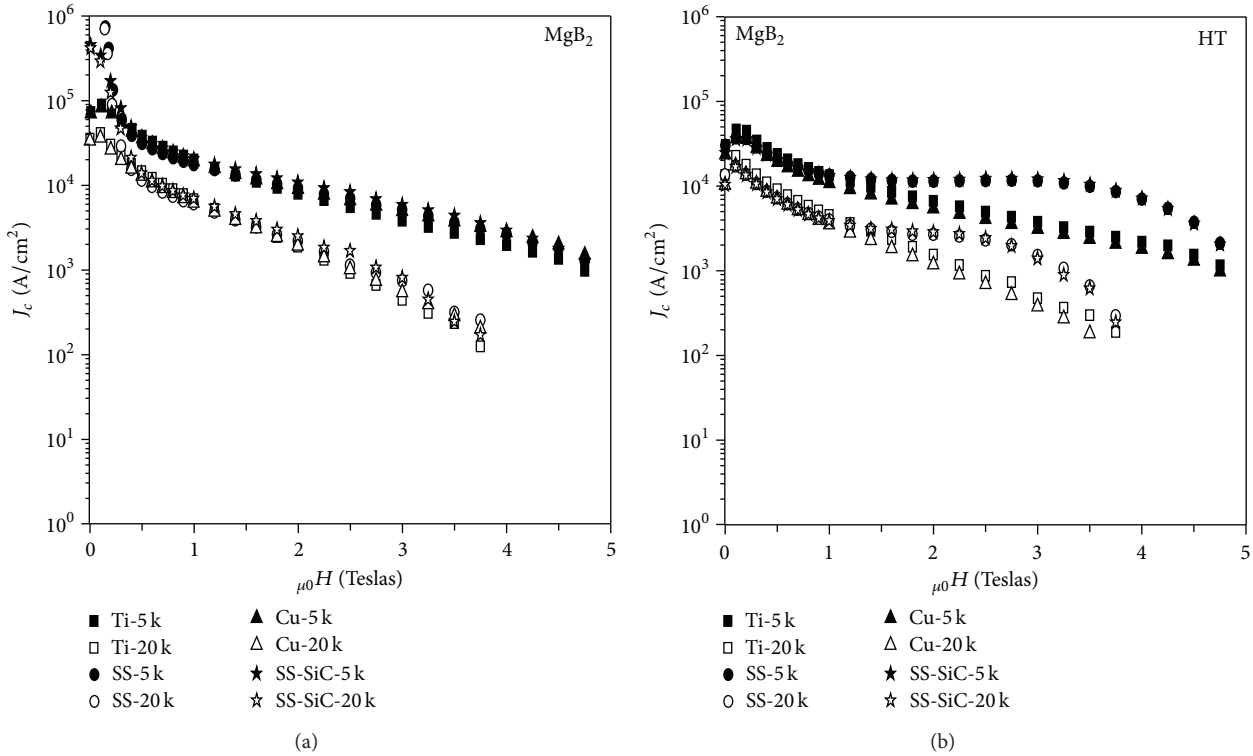

Figure 4: Magnetic J_c measurement of the MgB_2 superconducting wires: (a) Ti, Cu, SS, and SS-SiC before HT and (b) Ti, Cu, SS, and SS-SiC after HT.

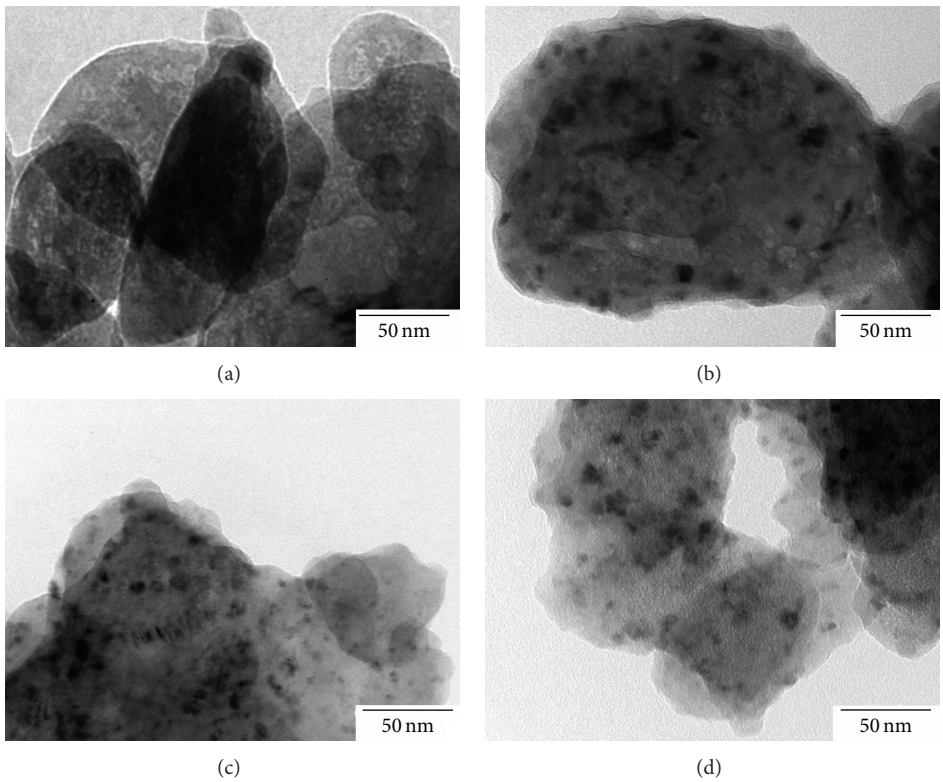

Figure 5: TEM micrographs of the HT wires: (a) Cu, (b) Ti, (c) SS, and (d) SS-SiC.

The higher density of precipitates on the powders from the SS and SS-SiC wires could be the reason of the improvement in J_c response of these wires at 5 and 20 K due to a better vortex pinning.

4. Conclusions

We fabricated ex situ MgB_2 monofilamentary wires using 3 different sheaths copper, stainless steel 316, and titanium grade 2 (Ti). None of them presented any reaction layer with the superconducting core. Stainless steel 316 wires show a better connectivity between grains and less pores than the others. An improvement on the J_c of SS wires is achieved. The J_c shows a plateau with values around 10^4 A/cm^2 and 10^3 A/cm^2 for 5 and 20 K on the SS wires. This enhancement is attributed to the presence of small $Mg(B,O)_2$ type precipitates distributed on the superconducting core of the SS wires.

Conflict of Interests

The authors declare that there is no conflict of interests regarding the publication of this paper.

References

[1] J. Nagamatsu, N. Nakagawa, T. Muranaka, Y. Zenitani, and J. Akimitsu, "Superconductivity at 39 K in magnesium diboride," *Nature (London)*, vol. 410, no. 6824, pp. 63–64, 2001.

[2] A. Serquis, L. Civale, D. L. Hammon et al., "Role of excess Mg and heat treatments on microstructure and critical current of MgB2 wires," *Journal of Applied Physics*, vol. 94, no. 6, pp. 4024–4031, 2003.

[3] X. Z. Liao, A. Serquis, Y. T. Zhu et al., "$Mg(B,O)_2$ precipitation in MgB_2," *Journal of Applied Physics*, vol. 93, pp. 6208–2615, 2003.

[4] V. Braccini, A. Malagoli, A. Tumino et al., "Improvement of magnetic field behavior of ex-situ processed magnesium diboride tapes," *IEEE Transactions on Applied Superconductivity*, vol. 17, no. 2, pp. 2766–2769, 2007.

[5] B. J. Senkowicz, R. Pérez Moyet, R. J. Mungall et al., "Atmospheric conditions and their effect on ball-milled magnesium diboride," *Superconductor Science and Technology*, vol. 19, no. 11, pp. 1173–1177, 2006.

[6] M. T. Malachevsky, A. C. Serquis, G. Serrano, J. P. M. Arias, G. Giunchi, and E. Perini, "Effect of the powder strain state on the mechanical properties of MgB_2 tapes," *IEEE Transactions on Applied Superconductivity*, vol. 21, no. 3, pp. 2676–2679, 2011.

[7] M. T. Malachevsky, J. M. Espasandin, A. C. Serquis, G. Serrano, and S. Dutrus, "Intensive milling effect on the properties of MgB_2 tapes," *IEEE Transactions on Applied Superconductivity*, vol. 19, no. 3, pp. 2730–2734, 2009.

[8] C. P. Bean, "Magnetization of hard superconductors," *Physical Review Letters*, vol. 8, no. 6, pp. 250–253, 1962.

[9] S. X. Dou, S. Soltanian, J. Horvat et al., "Enhancement of the critical current density and flux pinning of MgB_2 superconductor by nanoparticle SiC doping," *Applied Physics Letters*, vol. 81, pp. 3419–3421, 2002.

[10] P. Kováč, I. Hušek, T. Melišek, E. Martínez, and M. Dhalle, "Properties of doped *ex* and *in situ* MgB_2 multi-filament superconductors," *Superconductor Science and Technology*, vol. 19, no. 10, pp. 1076–1082, 2006.

[11] A. Serquis, L. Civale, D. L. Hammon, G. Serrano, and V. F. Nesterenko, "Optimization of critical currents in MgB_2 wires and coils," *IEEE Transactions on Applied Superconductivity*, vol. 15, pp. 3188–3191, 2005.

[12] W. K. Yeoh, J. H. Kim, J. Horvat et al., "Control of nano carbon substitution for enhancing the critical current density in MgB_2," *Superconductor Science and Technology*, vol. 19, no. 6, pp. 596–599, 2006.

[13] C. R. M. Grovenor, L. Goodsir, C. J. Salter, P. Kovac, and I. Husek, "Interfacial reactions and oxygen distribution in MgB_2 wires in Fe, stainless steel and Nb sheaths," *Superconductor Science and Technology*, vol. 17, no. 3, pp. 479–484, 2004.

[14] F. Sandiumenge, B. Martínez, and X. Obradors, "Tailoring of microstructure and critical currents in directionally solidified $YBa_2Cu_3O_{7-x}$," *Superconductor Science and Technology*, vol. 10, no. 7A, pp. A93–A119, 1997.

[15] X. Z. Liao, A. C. Serquis, Y. T. Zhu et al., "Controlling flux pinning precipitates during MgB_2 synthesis," *Applied Physics Letters*, vol. 80, no. 23, pp. 4398–4400, 2002.